

DiCoTTA: Domain-invariant Learning for Continual Test-time Adaptation

Sohyun Lee¹Nayeong Kim¹Juwon Kang¹Seong Joon Oh²Suha Kwak¹¹POSTECH²University of Tübingen

Abstract

This paper studies continual test-time adaptation (CTTA), the task of adapting a model to constantly changing unseen domains in testing while preserving previously learned knowledge. Existing CTTA methods mostly focus on adaptation to the current test domain only, overlooking generalization to arbitrary test domains a model may face in the future. To tackle this limitation, we present a novel online domain-invariant learning framework for CTTA, dubbed DiCoTTA. DiCoTTA aims to learn feature representation to be invariant to both current and previous test domains on the fly during testing. To this end, we propose a new model architecture and a test-time adaptation strategy dedicated to learning domain-invariant features without corrupting semantic contents, along with a new data structure and optimization algorithm for effectively managing information from previous test domains. DiCoTTA achieved state-of-the-art performance on four public CTTA benchmarks. Moreover, it showed superior generalization to unseen test domains.

1. Introduction

Deep neural networks have driven significant advances in various vision tasks such as classification [13, 24, 41], object detection [5, 6, 20], and semantic segmentation [9, 53, 73]. Despite these achievements, they often struggle with limited generalization ability to the domain shift between training and test data [4, 8, 18, 25, 37, 38, 57–59, 64]. Test-time adaptation (TTA) [30, 31, 48, 51, 52, 68, 76, 77] has been developed to mitigate the distribution shift by adapting a pre-trained model to unlabeled test domains during testing. In specific, TTA methods update the model in testing on the fly, by self-training using pseudo-labeled test data [17, 44, 62] or by entropy minimization of the model prediction [51, 68].

Early approaches to TTA assume a single and fixed test domain. In reality, however, this assumption does not hold since a model is often deployed in non-stationary and continually changing environments. In such environments, the accuracy of the model can easily degrade even with TTA since the constant distribution shift in testing causes unreliable pseudo labels [22], which in turn exacerbates error

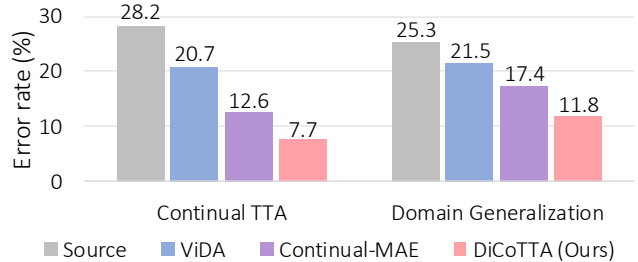


Figure 1. The effect of domain-invariant learning of DiCoTTA on CIFAR10-C. DiCoTTA demonstrates superior performance in domain generalization (DG) as well as continual test-time adaptation (CTTA), where the DG performance is evaluated on 5 unseen domains after CTTA over 10 domains.

accumulation and catastrophic forgetting.

Continual test-time adaptation (CTTA) [17, 35, 43, 44, 62, 71, 74, 75, 82] has been studied to address these realistic TTA scenarios. Most of existing CTTA methods focus only on adapting a model to the test domain at hand. Although these methods lead to notable performance improvements, there remains room for further improvement in that they do not consider the model’s generalization to future test domains it encounters later in continuously changing environments.

In this paper, we present an online Domain-invariant learning framework for Continual Test-Time Adaptation, dubbed DiCoTTA. DiCoTTA overcomes the aforementioned limitation by learning domain-invariant representations that well generalize to unseen domains on the fly during testing. This approach improves robustness of a model to arbitrary test domains that it may encounter in the future, as demonstrated in Fig. 1. A naïve approach to implementing domain-invariant learning is to align features from different test domains. However, since the features contain their own semantic contents as well as domain-specific information, this alignment without consideration of semantics corrupts the features and consequently degrades performance.

Hence, we introduce *domain information extractor* that takes the encoder features as input and extracts only domain-specific information in the form of embedding vectors; we call such vectors *domain embeddings*. The encoder is, in turn, trained to make domain embeddings from different

domains indistinguishable by reducing the gap between such domain embeddings, so that it learns domain-invariant representation. Analogous to adversarial learning [18, 21, 42], we alternate the optimization of the domain information extractor and that of the encoder. This approach allows the encoder to gradually become domain-invariant, and the domain information extractor to become sensitive to the remaining domain-specific information of the encoder.

The main challenge in implementing the idea above is that only the test domain at hand is accessible at each iteration of CTTA, while domain-invariant learning demands domain embeddings of at least two test domains. To tackle this, DiCoTTA efficiently stores embedding vectors that represent domain embeddings of the previous test domain; we call such embedding vectors *domain prototypes* and sample them from domain embeddings of the previous domain through submodular optimization [32, 50]. By ensuring that domain embeddings of the current domain are not distinguished from the domain prototypes of the previous domain, DiCoTTA performs domain-invariant learning of the encoder without access to samples of previous test domains.

DiCoTTA was evaluated on the four public benchmarks for CTTA: CIFAR10-to-CIFAR10-C [25, 34], CIFAR100-to-CIFAR100-C [25, 34], ImageNet-to-ImageNet-C [12, 25], and Cityscapes-to-ACDC [11, 60]. It achieved a new state of the art on all the benchmarks and demonstrated greater generalization ability on unseen test domains. The contribution of this paper is three-fold:

- We propose a new approach to CTTA that learns generalizable features to unseen domains for improving robustness on arbitrary test domains that a model may face in the future.
- We introduce a novel framework, dubbed DiCoTTA, that learns domain-invariant features during testing without access to previous test domains.
- DiCoTTA achieved the state of the art on four public benchmarks and demonstrated great generalization ability on unseen test data.

2. Related work

2.1. Test-time adaptation

Recent research on TTA aims at addressing the domain shift problem by adapting a pre-trained model online during testing [44, 65, 68, 71, 76, 77]. Initial studies [46, 65] employed self-supervised learning with proxy tasks on unlabeled test data, but they require modifications to the training stage to accommodate the proxy tasks. Meanwhile, Tent [68], a fully test-time adaptation method based on entropy minimization, requires no modifications to the training stage and is applicable to any pre-trained model. Building on this work, several studies [51, 52] have proposed using entropy-based losses in testing environments: EATA [51] utilizes the

entropy loss only for reliable samples, while SAR [52] incorporates a sharpness-aware entropy loss to achieve smooth loss landscapes, which are known to improve generalization [7, 16, 70]. Other approaches [15, 30, 46, 63] leveraged lightweight information from source data to facilitate adaptation while mitigating catastrophic forgetting. For example, TTT++ [46] stores mean and covariance matrices, while TTAC [63] stores category-wise features of source data to align feature distributions during testing. Unlike these methods, our method does not require any computation for source data. Instead, it directly extracts domain embeddings from streamed test data, enabling domain-invariant learning during testing.

2.2. Continual test-time adaptation

In real-world scenarios, testing environments can vary significantly due to multiple factors such as weather, time, and geolocation. Since conventional TTA methods have been studied under the assumption that the test domain is static, they face challenges in continually changing environments. To address this limitation, Wang *et al.* [71] introduced the first CTTA method, leveraging multiple augmented inputs and a momentum network to generate more reliable pseudo labels. Song *et al.* [62] and Lee *et al.* [35] proposed memory-efficient methods that utilized lightweight meta networks and a mixture of experts, respectively. VDP [17] and ViDA [44] utilized visual prompt learning and visual domain adapters, respectively, to disentangle domain-specific and domain-shared knowledge. Continual-MAE [43] improved target domain knowledge extraction through a self-supervised framework. In this context, Yang *et al.* [75] proposed a versatile network that identifies and refines unreliable pseudo-labels using the source pre-trained model, while Zhu *et al.* [82] introduced an uncertainty-aware buffering and graph-based constraint. Unlike these methods, DiCoTTA learns domain-invariant features that well generalize to diverse unseen test domains.

2.3. Domain generalization

Domain generalization (DG) focuses on improving the generalization performance of models on unseen target domains by training them with multiple source domains. Initial work in DG employed domain alignment [28, 40, 42, 61, 72] to learn domain-invariant representations by minimizing the distance of distribution among multiple domains. Recent studies in DG have introduced various strategies, including data augmentation [29, 78, 79], meta learning [3, 14], and representation learning [23, 49]. Inspired by DG, this paper presents a CTTA method that updates an online model through domain-invariant learning to handle continually changing domains.

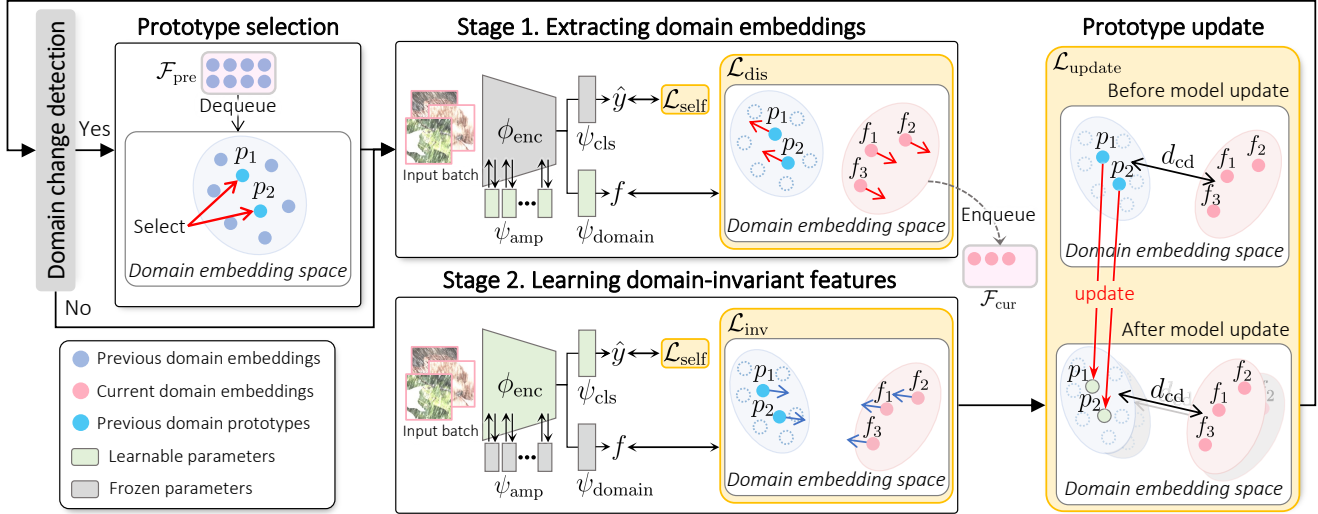


Figure 2. Overview of DiCoTTA. When a domain change is detected, DiCoTTA selects domain prototypes that well represent the previous domain embeddings stored in a queue. Stages 1 and 2 are alternated in each iteration. In Stage 1, the domain information extractor ψ_{domain} learns alongside domain amplifier ψ_{amp} to extract domain embeddings from the encoder features using the domain discrimination loss \mathcal{L}_{dis} . In Stage 2, the encoder ϕ_{enc} is trained using the domain-invariant loss \mathcal{L}_{inv} to reduce the gap between domain embeddings and domain prototypes of the previous domain. The domain prototypes are continuously updated to match with the updated model parameters by $\mathcal{L}_{\text{update}}$.

3. Proposed method

DiCoTTA is an online domain-invariant learning framework for CTTA; its overall pipeline is illustrated in Fig. 2, and the algorithm detailed in Sec. A of the supplement. Unlike domain adaptation and generalization, which in general assume that data from at least two domains are available during the entire training process, CTTA allows access to a handful of data from the test domain at hand (*i.e.*, the input data at each test point) for each iteration. This constraint poses a non-trivial challenge for domain-invariant learning.

DiCoTTA addresses this challenge by storing *domain embeddings*, *i.e.*, embedding vectors containing domain information of the most recent previous domain, in a queue. To prevent excessive memory consumption caused by storing all domain embeddings, we select representative embeddings from the queue of domain embeddings as domain prototypes when the test domain changes.

To achieve domain-invariant learning without corrupting the semantics of features, DiCoTTA operates in two stages as follows. In the first stage, the domain information extractor learns to extract domain embeddings, by capturing only domain-specific information from the encoder features. To facilitate this extraction, another extra module called *domain amplifier* is attached to the encoder for capturing and emphasizing the domain-specific information of the encoder features. We design the domain amplifier as a lightweight adapter structure [10, 27, 55] to minimize additional parameters; details of the structure are provided in Sec. B.2 of the supplement. During this stage, the domain amplifier is

updated alongside the domain information extractor while the encoder remains frozen. In the second stage, we perform domain-invariant learning by ensuring the domain embeddings of the current domain become indistinguishable from the domain prototypes of the previous domain. During this stage, only the encoder is updated, with the domain information extractor and domain amplifier frozen.

By alternating between the two stages, the encoder gradually learns domain-invariant features across multiple test domains. Meanwhile, the domain information extractor and domain amplifier are updated to reflect the update of the encoder and extract domain embeddings corresponding to the current state of the encoder. In addition, DiCoTTA continuously updates the domain prototypes to match them with the updated model parameters. Since the model used to extract domain prototypes is constantly updated during CTTA, the prototypes must also be updated accordingly.

The remainder of this section elaborates on domain change detection (Sec. 3.1), domain prototype selection (Sec. 3.2), the two-stage process of domain-invariant learning (Sec. 3.3), and domain prototype update (Sec. 3.4).

3.1. Domain change detection

As it is unknown when the test domain changes in CTTA, we detect domain changes based on prediction confidence scores as in [17]. That is, if the difference between confidence scores of two consecutive predictions is greater than a threshold, the test domain is considered to have changed. DiCoTTA is designed to remain effective even with detection errors: false positives are caused by intra-domain shifts and

thus let DiCoTTA learn invariant features within a single domain, while false negatives suggest mild distribution shifts that can be handled robustly by the model at hand as-is.

3.2. Domain prototype selection

When a domain change is detected, DiCoTTA retains a small set of n domain prototypes $\mathcal{P}_{\text{pre}} = \{p_i\}_{i=1}^n$ from the previous domain embeddings in the queue $\mathcal{F}_{\text{pre}} = \{f_i\}_{i=1}^m$ to reduce memory footprint substantially. To ensure that these prototypes represent the entire distribution of the previous domain, we select \mathcal{P}_{pre} by minimizing the discrepancy between \mathcal{F}_{pre} and \mathcal{P}_{pre} . Following the prototype sampling technique [32], we measure the discrepancy between \mathcal{F}_{pre} and \mathcal{P}_{pre} using the squared maximum mean discrepancy (MMD):

$$\begin{aligned} \text{MMD}^2(\mathcal{F}_{\text{pre}}, \mathcal{P}_{\text{pre}}) &:= \frac{1}{|\mathcal{F}_{\text{pre}}|^2} \sum_{f_i, f_j \in \mathcal{F}_{\text{pre}}} k(f_i, f_j) \\ &\quad - \frac{2}{|\mathcal{F}_{\text{pre}}||\mathcal{P}_{\text{pre}}|} \sum_{f_i \in \mathcal{F}_{\text{pre}}, p_j \in \mathcal{P}_{\text{pre}}} k(f_i, p_j) \\ &\quad + \frac{1}{|\mathcal{P}_{\text{pre}}|^2} \sum_{p_i, p_j \in \mathcal{P}_{\text{pre}}} k(p_i, p_j), \end{aligned} \quad (1)$$

where $k(\mathbf{x}, \mathbf{x}') = \exp(-\gamma\|\mathbf{x} - \mathbf{x}'\|^2)$ is a RBF kernel that measures the discrepancy between embeddings from the two sets. As the first term in Eq. (1) remains constant with respect to \mathcal{P}_{pre} , we define a score function $J(\mathcal{P}_{\text{pre}})$ as follows:

$$\begin{aligned} J(\mathcal{P}_{\text{pre}}) &:= \text{MMD}^2(\mathcal{F}_{\text{pre}}, \emptyset) - \text{MMD}^2(\mathcal{F}_{\text{pre}}, \mathcal{P}_{\text{pre}}) \\ &= \frac{2}{|\mathcal{F}_{\text{pre}}||\mathcal{P}_{\text{pre}}|} \sum_{f_i \in \mathcal{F}_{\text{pre}}, p_j \in \mathcal{P}_{\text{pre}}} k(f_i, p_j) \\ &\quad - \frac{1}{|\mathcal{P}_{\text{pre}}|^2} \sum_{p_i, p_j \in \mathcal{P}_{\text{pre}}} k(p_i, p_j), \end{aligned} \quad (2)$$

where the constant term $\text{MMD}^2(\mathcal{F}_{\text{pre}}, \emptyset)$ is added to ensure that $J(\emptyset) = 0$. The domain prototypes are selected by maximizing the score function:

$$\max_{\mathcal{P}_{\text{pre}} \subset \mathcal{F}_{\text{pre}}: |\mathcal{P}_{\text{pre}}|=n} J(\mathcal{P}_{\text{pre}}). \quad (3)$$

This optimization is generally intractable, but a near-optimal solution can be achieved through a greedy process since the function J is normalized monotone submodular [50] when using the RBF kernel for $k(\cdot, \cdot)$, as proved in [32]. By maximizing the score function $J(\mathcal{P}_{\text{pre}})$, selected prototypes closely approximate the entire distribution of domain embeddings in the queue. At the initial stage where no previous test domain exists, we use domain embeddings of augmented test images as domain prototypes.

3.3. Domain-invariant learning

DiCoTTA updates the model through domain-invariant learning and self-training. For domain-invariant learning, we

employ a two-stage process. In the first stage, the domain information extractor and amplifier are updated to extract domain-specific information, *i.e.*, domain embeddings, from the encoder features. In the second stage, the encoder is updated to be domain-invariant by aligning the current domain embeddings with the previous domain prototypes (Sec. 3.2). Alternating these two stages allows the encoder to gradually become domain-invariant, and the domain information extractor and amplifier to become sensitive to the remaining domain-specific information of the encoder. In addition, following previous work [17, 44, 71], we update our model by a self-training loss $\mathcal{L}_{\text{self}}$, a cross-entropy loss between our model’s prediction \hat{y} and a pseudo label \tilde{y} generated by its exponential moving average [66]:

$$\mathcal{L}_{\text{self}}(x) = -\frac{1}{C} \sum_{c=1}^C \tilde{y}_c \log \hat{y}_c, \quad (4)$$

where C is the total number of classes. For inference, we use \hat{y} as the classification prediction. Details of the two stages are described below.

Stage 1: Extracting domain embeddings. To maintain the semantic information of the encoder features during domain-invariant learning, we first extract their domain-specific information in the form of embedding vectors. To this end, we introduce the domain information extractor that extracts domain embeddings from output features of the encoder, and the domain amplifier that amplifies the domain-specific information of the encoder to facilitate the extractor. Let $\mathcal{F}_{\text{cur}} = \{f_i\}_{i=1}^n$ be the domain embeddings of test input images from the current test domain and \mathcal{P}_{pre} the previous domain’s prototypes. The domain information extractor and amplifier learn a domain embedding space by distinguishing \mathcal{F}_{cur} and \mathcal{P}_{pre} with a domain discrimination loss:

$$\begin{aligned} \mathcal{L}_{\text{dis}}(\mathcal{F}_{\text{cur}}, \mathcal{P}_{\text{pre}}) &= \\ &= -\frac{1}{n} \left\{ \sum_{f_i \in \mathcal{F}_{\text{cur}}} \log(D(f_i)) - \sum_{p_i \in \mathcal{P}_{\text{pre}}} \log(1 - D(p_i)) \right\}, \end{aligned} \quad (5)$$

where $D(\cdot)$ indicates a binary linear classifier that serves as a domain discriminator. Minimizing this loss encourages the domain extractor with the amplifier to learn a space where embeddings of different domains are separated and thus capture domain-specific information [37, 47].

Stage 2: Learning domain-invariant features. The second stage aims to optimize the encoder to achieve domain invariance across diverse test domains alongside classification (Eq. 4). DiCoTTA accomplishes this by aligning the current domain embeddings and the previous domain’s prototypes. To be specific, we update the encoder and its classification head while freezing the domain information extractor and amplifier. Given current domain embeddings \mathcal{F}_{cur} and previous domain prototypes \mathcal{P}_{pre} , the domain-invariant learning

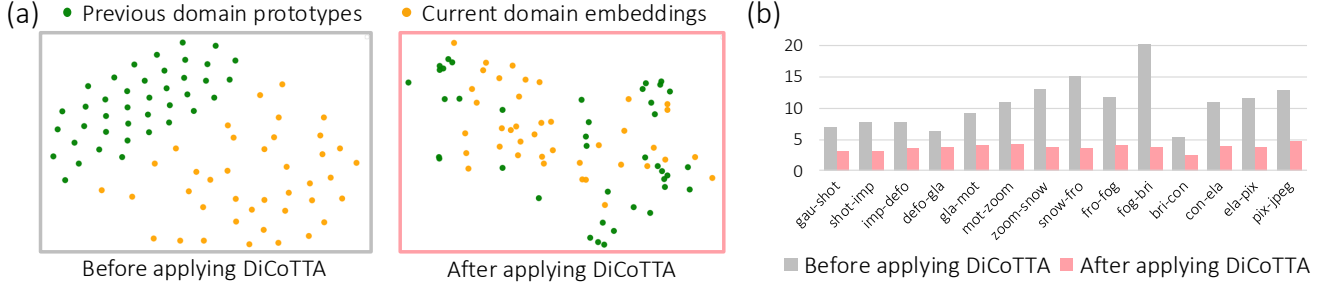


Figure 3. Empirical analysis on the impact of domain-invariant learning in DiCoTTA. (a) 2D visualization of the distribution of domain embeddings from different domains before and after DiCoTTA. (b) The domain gap between different domains measured by Chamfer distance before and after applying DiCoTTA.

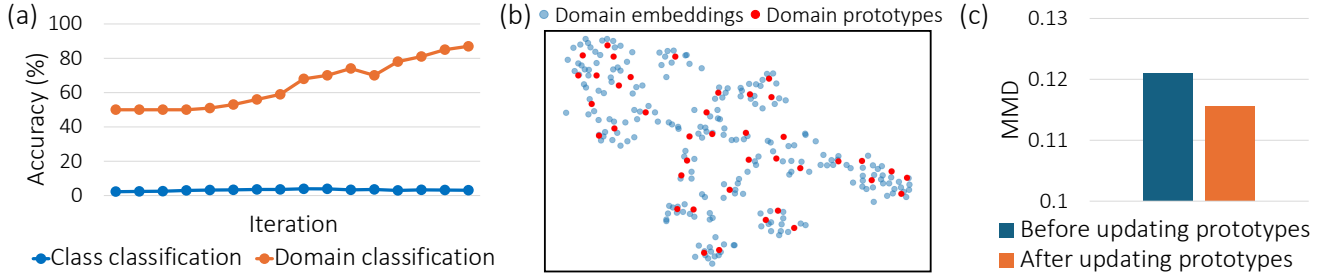


Figure 4. Empirical analysis on domain embeddings and prototypes. (a) Analysis of class classification and domain classification accuracy using domain embeddings during CTTA iterations. (b) 2D visualization of domain embeddings and domain prototypes. (c) MMD between the target and original prototypes before the update and that between the target and updated prototypes.

loss is given by

$$\mathcal{L}_{\text{inv}}(\mathcal{F}_{\text{cur}}, \mathcal{P}_{\text{pre}}) = \frac{1}{n} \sum_{(f_i, p_i) \in (\mathcal{F}_{\text{cur}}, \mathcal{P}_{\text{pre}})} \|f_i - p_i\|_1. \quad (6)$$

By minimizing this loss, the encoder’s features are trained to produce domain embeddings that are indistinguishable between different domains, making them domain-agnostic and generalizable to future unseen domains.

3.4. Domain prototype update

Since the model used to extract the domain prototypes is constantly updated during CTTA, the domain prototypes extracted from the earlier model become outdated. Thus, the domain prototypes should also be updated to reflect the update of the model, approximating prototypes extracted from the updated model. Inspired by Asadi *et al.* [2], we aim to preserve the set similarity between the previous domain prototypes \mathcal{P}_{pre} and the current domain embeddings \mathcal{F}_{cur} to effectively keep the relationship between them intact. In specific, we measure the Chamfer distance between the two sets \mathcal{P}_{pre} and \mathcal{F}_{cur} . For iteration t , we update the domain prototypes $\mathcal{P}_{\text{pre}}^{t-1}$ to $\mathcal{P}_{\text{pre}}^t$ to ensure that the Chamfer distance between previous domain prototypes and current domain embeddings remains consistent before and after the model update. Specifically, the domain prototypes $\mathcal{P}_{\text{pre}}^t$ are updated

by minimizing the prototype updating loss:

$$\mathcal{L}_{\text{update}} = |d_{\text{CD}}(\mathcal{F}_{\text{cur}}^{t-1}, \mathcal{P}_{\text{pre}}^{t-1}) - d_{\text{CD}}(\mathcal{F}_{\text{cur}}^t, \mathcal{P}_{\text{pre}}^t)|, \quad (7)$$

where the Chamfer distance d_{CD} is computed by

$$d_{\text{CD}}(\mathcal{F}_{\text{cur}}, \mathcal{P}_{\text{pre}}) = \sum_{f_i \in \mathcal{F}_{\text{cur}}} \min_{p_j \in \mathcal{P}_{\text{pre}}} \|p_j - f_i\|_2^2 + \sum_{p_j \in \mathcal{P}_{\text{pre}}} \min_{f_i \in \mathcal{F}_{\text{cur}}} \|p_j - f_i\|_2^2. \quad (8)$$

3.5. Empirical justification

Domain-invariant learning. We analyze the impact of domain-invariant learning both qualitatively and quantitatively. Fig. 3(a) provides a t -SNE visualization [67] of domain embeddings from different domains (*i.e.*, Gaussian and Shot noise) before and after applying DiCoTTA, demonstrating that DiCoTTA effectively reduces the gap between different domains. In Fig. 3(b), we quantitatively measured the Chamfer distance between domain embeddings from different domains before and after applying DiCoTTA. This result indicates that the distance decreases as intended after the domain-invariant learning.

Domain embedding. In Fig. 4(a), we empirically verify that domain embeddings capture domain-specific information more prominently than content information. To assess

Method	gaussian	shot	impulse	defocus	glass	motion	zoom	snow	frost	fog	brightness	contrast	elastic_trans	pixelate	jpeg	Mean↓	Gain
Source [13] ICLR2021	60.1	53.2	38.3	19.9	35.5	22.6	18.6	12.1	12.7	22.8	5.3	49.7	23.6	24.7	23.1	28.2	/
Pseudo [36] ICML2013	59.8	52.5	37.2	19.8	35.2	21.8	17.6	11.6	12.3	20.7	5.0	41.7	21.5	25.2	22.1	26.9	+1.3
TENT [69] ICLR2021	57.7	56.3	29.4	16.2	35.3	16.2	12.4	11.0	11.6	14.9	4.7	22.5	15.9	29.1	19.5	23.5	+4.7
CoTTA [71] CVPR2022	58.7	51.3	33.0	20.1	34.8	20.0	15.2	11.1	11.3	18.5	4.0	34.7	18.8	19.0	17.9	24.6	+3.6
VDP [17] AAAI2023	57.5	49.5	31.7	21.3	35.1	19.6	15.1	10.8	10.3	18.1	4.0	27.5	18.4	22.5	19.9	24.1	+4.1
ViDA [44] ICLR2024	52.9	47.9	19.4	11.4	31.3	13.3	7.6	7.6	9.9	12.5	3.8	26.3	14.4	33.9	18.2	20.7	+7.5
Continual-MAE [43] CVPR2024	30.6	18.9	11.5	10.4	22.5	13.9	9.8	6.6	6.5	8.8	4.0	8.5	12.7	9.2	14.4	12.6	+15.6
Yang <i>et al.</i> [75] CVPR2024	16.3	11.1	9.6	8.4	14.6	8.6	5.5	6.3	5.7	7.1	3.3	5.4	10.9	7.7	12.8	8.9	+19.3
DiCoTTA	17.4	10.9	5.4	6.3	16.3	6.9	3.9	3.7	3.8	5.9	2.2	4.7	7.8	11.2	9.4	7.7	+20.5

Table 1. Classification error rates (%) on CIFAR10-to-CIFAR10-C online CTTA task. Gain (%) represents the percentage of improvement in accuracy compared with the source method.

the content information within the domain embeddings, we performed linear probing by training a linear classification layer using the domain embeddings as input while keeping the model frozen. The results show that domain classification using the domain embeddings consistently achieves higher accuracy than class classification, indicating that the domain embeddings predominantly encode domain-specific information with minimal content information, as intended.

Domain prototype selection. We qualitatively investigate how well domain prototypes represent the entire set of domain embeddings. Fig. 4(b) provides a *t*-SNE visualization of domain embeddings and selected domain prototypes, specifically conducted on the Gaussian noise domain. This visualization demonstrates that our domain prototypes are selected to be diverse and well represent the overall distribution of the domain embeddings.

Domain prototype update. Fig. 4(c) demonstrates the effectiveness of the prototype updating strategy. By forwarding the corresponding images of each prototype through the updated model, we obtain target prototypes that represent the desired prototype representations in the updated feature space. The MMD value between these target prototypes and our updated prototypes is lower than those between target prototypes and original prototypes, where MMD values are averaged across all CTTA steps. This result validates that our prototype updating method effectively moves the prototypes toward their targeted representations.

4. Experiments

4.1. Experimental setting

Evaluation benchmarks. Our method was evaluated on both classification and semantic segmentation tasks. For classification, we utilized three benchmarks [25]: CIFAR10-C, CIFAR100-C, and ImageNet-C, each consisting of 15 corruption types and five severity levels. We reported the results for the most severe level (level 5). For segmentation, we used the Cityscapes dataset [11] as the source dataset and the ACDC dataset [60] as the test dataset, including four

unseen test domains: Fog, Night, Rain, and Snow.

Evaluation scenario. Following Wang *et al.* [71], DiCoTTA was evaluated under an online CTTA setting where the prediction is assessed immediately after data are streamed, and the pre-trained model is adapted on the fly. For the segmentation task, the test domains are repeated cyclically for three rounds. Additionally, we evaluated the generalization ability to unseen domains on CIFAR10-C using the leave-one-domain-out rule [39, 44, 80], applying CTTA methods to 10 domains of ImageNet-C and testing on the 5 unseen domains without any model adaptation. In line with recent CTTA studies [43, 44, 75], we reported results for all methods using a common ViT backbone. This follows the standardization introduced by ViDA [44], which established the use of ViTs in CTTA and re-implemented previous CNN-based methods within this ViT-based framework. For additional experiments beyond those reported by previous studies, we evaluated methods with publicly available code.

Implementation details. We utilized ViT-base [13] for classification tasks and Segformer-B5 [73] for the segmentation task as the backbone. Input images were resized to 224×224 for ViT-base and to 960×540 for Segformer-B5. The size of the queue storing the domain embeddings and domain prototypes was set to 256 and 40, respectively. The domain information extractor ψ_{domain} and domain discriminator D were both implemented as MLP whose activation functions are ReLU [1] and GELU [26], respectively. The domain amplifier was implemented as an adapter that includes an up-projection layer and a down-projection layer, with an intermediate dimension of 128. More details are given in Sec. B.1 of the supplement.

4.2. Evaluation on classification tasks

To evaluate the performance of DiCoTTA, we conducted extensive experiments on three conventional benchmarks: CIFAR10-C, CIFAR100-C, and ImageNet-C.

Performance on corruption benchmarks. Table 1 and Table a3 present the results on CIFAR10-C and CIFAR100-C, respectively. DiCoTTA significantly outperformed all

Method	Mean↓	Gain	Method	Mean↓	Gain
Source [13]	35.4	/	Source [13]	55.8	/
Pseudo [36]	33.2	+2.2	Pseudo [36]	61.2	-5.4
TENT [69]	32.1	+3.3	TENT [69]	51.0	+4.8
CoTTA [71]	34.8	+0.6	CoTTA [71]	54.8	+1.0
VDP [17]	32.0	+3.4	VDP [17]	50.0	+5.8
ViDA [44]	27.3	+8.1	ViDA [44]	43.4	+12.4
Continual-MAE [43]	26.4	+9.0	Continual-MAE [43]	42.5	+13.3
Yang <i>et al.</i> [75]	24.0	+11.4	Yang <i>et al.</i> [75]	42.7	+13.1
DiCoTTA	23.3	+12.1	DiCoTTA	42.5	+13.3

Table 2. Classification error rates (%) on CIFAR100-to-CIFAR100-C online CTTA task.

Table 3. Classification error rates (%) on ImageNet-to-ImageNet-C online CTTA.

Backbone	Metric	Source [13]	TENT [36]	CoTTA [71]	ViDA [44]	DiCoTTA
DINOv2	Mean↓	25.0	21.7	29.3	20.2	13.5
	Gain	/	+3.3	-4.3	+4.8	+11.5
SAM	Mean↓	39.3	37.5	39.4	34.1	17.3
	Gain	/	+1.8	-0.1	+5.2	+22.0

Table 6. Average classification error rates (%) on CIFAR10-to-CIFAR10C CTTA task using pre-trained encoders from foundation models (DINOv2 and SAM).

other methods across various corruption types. Specifically, it achieved the lowest mean error rate of 7.7% on CIFAR10-C and 23.3% on CIFAR100-C, showing improvements of 20.5%p and 12.1%p over the source model, respectively. As shown in Table a6, DiCoTTA also achieved the best performance on the ImageNet-C dataset.

Generalization performance on unseen domains. Table 4 summarizes the classification error rates on 5 unseen domains of CIFAR10-C after CTTA over 10 domains. DiCoTTA achieved the lowest mean error rate, highlighting the benefit of domain-invariant learning and demonstrating its generalization ability by maintaining robustness even on unseen domains. This indicates that DiCoTTA not only adapts well to continually changing domains but also generalizes effectively to unseen domains.

Gradually changing results. Table 5 shows results of continual test-time adaptation on a CIFAR10-C gradually changing setup [71], where the corruption types changed gradually over time. DiCoTTA still demonstrated superior performance, notably outperforming existing methods.

Continual adapting for foundation models. Foundation models trained on large-scale datasets possess powerful generalization capabilities, but adapting them to downstream datasets can further improve their performance on target tasks [45, 56, 81]. To evaluate the effectiveness of our method on foundation models, we applied DiCoTTA to DINOv2 [54], a representative image-level foundation model, and SAM [33], a pixel-level foundation model, under continually changing test domains. Following the experimental setting of ViDA [44], we treated these foundation models as pre-trained models and applied each CTTA method to them

Method	brightness	contrast	elastic_trans	pixelate	jpeg	Mean↓	Gain
Source [13]	5.3	49.7	23.6	24.7	23.1	25.3	/
ViDA [44]	4.1	36.4	15.6	33.5	17.8	21.5	+3.8
Continual-MAE [43]	5.0	25.7	15.1	22.6	18.7	17.4	+7.9
DiCoTTA	2.5	12.6	12.8	18.7	12.6	11.8	+13.5

Table 4. Generalization performance evaluated by error rates (%) on 5 unseen CIFAR10-C domains after applying CTTA over 10 other domains.

	Source [13]	ViDA [44]	Continual-MAE [43]	DiCoTTA
Mean↓	13.7	7.7	6.5	3.6
Gain	/	+6.0	+7.2	+10.1

Table 5. CTTA results under gradual domain shifts on CIFAR10-to-CIFAR10-C, evaluated by error rates (%).

on CIFAR10-C. Table 6 shows the results, demonstrating that our method enhanced the performance of both models and enabled continual adaptation without degradation.

4.3. Evaluation on segmentation tasks

Table 7 presents the segmentation results from adapting Cityscapes to ACDC, a real-world adverse condition dataset. Across three rounds, DiCoTTA consistently achieved the highest mIoU among existing CTTA methods. In the first round, our method reached an average mIoU of 62.0%, representing a 5.3%p gain over the source model. In subsequent rounds, DiCoTTA performed strongly on newly encountered domains while preserving robustness on previously encountered domains, effectively handling continually changing environments. These results suggest that DiCoTTA successfully mitigates domain shifts in semantic segmentation tasks, maintaining robustness across diverse and real-world adverse conditions. Further analyses are given in Sec. E.1 and F.3.

4.4. In-depth analysis

Impact of domain amplifier. We investigated the impact of the domain amplifier by evaluating DiCoTTA with and without the domain amplifier by comparing their error rates (Table 8) and attention maps derived from the final Transformer block (Fig. 5). Removing the amplifier substantially increased error rates and produced less reliable attention maps. The results show that the domain amplifier plays a crucial role in DiCoTTA, extracting domain-specific information from each layer of the encoder, thereby enabling the encoder to become domain-invariant.

Ablation study of each loss. We conducted an ablation study to evaluate the contributions of each loss component in our method. The results, presented in Table 9, demonstrate that each loss contributes to the overall performance improvement. Notably, the domain-invariant learning loss \mathcal{L}_{inv} was crucial for achieving high performance by guiding the model to learn domain-invariant features, which are essential for effective adaptation across different domains. Additionally, the domain discrimination loss \mathcal{L}_{dis} , which facilitated the learning of domain embeddings, was also crucial for

Time	$t \longrightarrow$															
Round	1					2					3					Mean \uparrow
Method	Fog	Night	Rain	Snow	Mean \uparrow	Fog	Night	Rain	Snow	Mean \uparrow	Fog	Night	Rain	Snow	Mean \uparrow	Mean \uparrow
Source [73] ICLR2021	69.1	40.3	59.7	57.8	56.7	69.1	40.3	59.7	57.8	56.7	69.1	40.3	59.7	57.8	56.7	56.7
TENT [69] ICLR2021	69.0	40.2	60.1	57.3	56.7	68.3	39.0	60.1	56.3	55.9	67.5	37.8	59.6	55.0	55.0	55.7
CoTTA [71] CVPR2022	70.9	41.2	62.4	59.7	58.6	70.9	41.1	62.6	59.7	58.6	70.9	41.0	62.7	59.7	58.6	58.6
DePT [19] arXiv	71.0	40.8	58.2	56.8	56.5	68.2	40.0	55.4	53.7	54.3	66.4	38.0	47.3	47.2	49.7	53.4
ECoTTA [62] CVPR2023	68.5	35.8	62.1	57.4	56.0	68.3	35.5	62.3	57.4	55.9	68.1	35.3	62.3	57.3	55.8	55.8
VDP [17] AAAI2023	70.5	41.1	62.1	59.5	58.3	70.4	41.1	62.2	59.4	58.2	70.4	41.0	62.2	59.4	58.2	58.2
ViDA [44] ICLR2024	71.6	43.2	66.0	63.4	61.1	73.2	44.5	67.0	63.9	62.2	73.2	44.6	67.2	64.2	62.3	61.9
BECoTTA [35] ICML2024	72.3	42.0	63.5	60.1	59.5	72.4	41.9	63.5	60.2	59.5	72.3	41.9	63.6	60.2	59.5	59.5
SVDP [74] AAAI2024	72.1	44.0	65.2	63.0	61.1	72.2	44.5	65.9	63.5	61.5	72.1	44.2	65.6	63.6	61.4	61.3
Continual-MAE [43] CVPR2024	71.9	44.6	67.4	63.2	61.8	71.7	44.9	66.5	63.1	61.6	72.3	45.4	67.1	63.1	62.0	61.8
Zhu <i>et al.</i> [82] ECCV2024	71.2	42.3	64.9	62.0	60.1	72.6	43.2	66.3	63.2	61.3	72.8	43.8	66.5	63.2	61.6	61.0
DiCoTTA	71.9	45.5	66.4	63.9	62.0 ± 0.1	73.2	45.8	67.4	64.1	62.6 ± 0.1	72.8	44.7	67.9	63.7	62.3 ± 0.1	62.3 ± 0.1

Table 7. Segmentation results on Cityscape-to-ACDC online CTTA task. Mean is the average score of mIoU.

Error rate (%)		\mathcal{L}_{self}	\mathcal{L}_{inv}	\mathcal{L}_{dis}	$J(\mathcal{P}_{pre})$	\mathcal{L}_{update}	Mean \downarrow
(a) w/o ψ_{amp}	21.9						28.2
(b) w/ ψ_{amp}	7.7	✓	✓	✓	✓	✓	18.0
		✓	✓	✓	✓	✓	10.5
		✓	✓	✓	✓	✓	8.3
		✓	✓	✓	✓	✓	8.0
		✓	✓	✓	✓	✓	7.7

Table 8. Ablation study on ψ_{amp} .

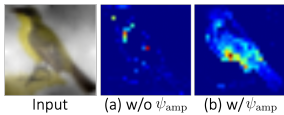


Figure 5. Impact of ψ_{amp} .

Table 9. Ablation study on each loss of DiCoTTA.

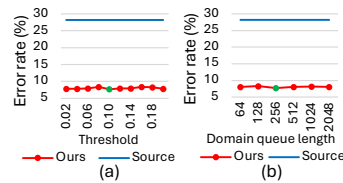


Figure 6. Sensitivity to hyperparameters. (a) Threshold for domain change detection. (b) Queue length.

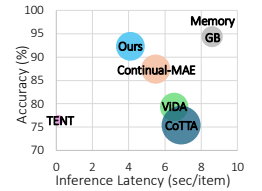


Figure 7. Comparison of computational cost on change detection. (a) Threshold for domain change detection. (b) Queue length. CIFAR10-C.

DiCoTTA. Furthermore, both the score function for domain prototype selection $J(\mathcal{P}_{pre})$ and the prototype updating loss \mathcal{L}_{update} contributed to the performance of DiCoTTA.

Sensitivity to the threshold for domain change detection.

To investigate the effect of the threshold used for domain change detection, we conducted experiments varying the threshold values. Fig. 6(a) summarizes the results for thresholds ranging from 0.02 to 0.20. The performance remained stable across this range of thresholds, consistently outperforming the source model. These results suggest that DiCoTTA is insensitive to threshold settings.

Sensitivity to the queue length $|\mathcal{F}_{pre}|$. We evaluated the impact of $|\mathcal{F}_{pre}|$, which specifies the length of the queue that stores previous domain embeddings. It is designed to retain a sufficient number of embeddings while minimizing the inclusion of excessively outdated information. Fig. 6(b) presents the error rates on CIFAR10-C for six different queue lengths. The results indicate that the error rates remain consistent across all tested values of $|\mathcal{F}_{pre}|$, demonstrating that DiCoTTA is insensitive to the length of the queue. An extended analysis is provided in Sec. C.3.

Comparison of computational cost. We evaluated the computational cost of DiCoTTA in terms of inference latency and memory consumption with the prediction accuracy. As shown in Fig. 7, while TENT [68] exhibited the highest computational efficiency, it had the lowest prediction accu-

racy among the evaluated methods. In contrast, DiCoTTA achieved reduced inference latency and comparable memory consumption compared to other CTTA methods (excluding TENT) while outperforming them in prediction accuracy.

5. Conclusion

We have introduced DiCoTTA, a novel online domain-invariant learning framework for CTTA. Unlike existing CTTA methods that focus only on adaptation to the current test domain and thus often lack generalization to arbitrary future test domains, DiCoTTA aims to learn domain-invariant features during testing through a carefully designed model architecture and test-time training strategy. Through extensive experiments, we have validated that DiCoTTA improves generalization to arbitrary unseen domains, ensures robust adaptation in dynamically changing test environments, and consequently achieves the best on all CTTA benchmarks.

Limitations and future work. DiCoTTA is less robust to initial corruptions due to limited exposure to diverse domain shifts as described in Sec. E.3, and we believe early adaptation strategies could mitigate this issue. Also, DiCoTTA currently uses only the most recent previous domain for domain-invariant learning, and incorporating additional previously encountered domains with minimal memory usage could further improve its performance.

Contents

1. Introduction	1
2. Related work	2
2.1. Test-time adaptation	2
2.2. Continual test-time adaptation	2
2.3. Domain generalization	2
3. Proposed method	3
3.1. Domain change detection	3
3.2. Domain prototype selection	4
3.3. Domain-invariant learning	4
3.4. Domain prototype update	5
3.5. Empirical justification	5
4. Experiments	6
4.1. Experimental setting	6
4.2. Evaluation on classification tasks	6
4.3. Evaluation on segmentation tasks	7
4.4. In-depth analysis	7
5. Conclusion	8
A Algorithm of DiCoTTA	9
B Experimental details	10
B.1. Implementation details	10
B.2. Structure of domain amplifier	10
C Additional ablation study	10
C.1. Ablation study on number of domain prototypes	10
C.2. Ablation study on distance metrics for proto- type update	10
C.3. Extended ablation study on thresholds	11
D Empirical analysis	11
D.1. Empirical analysis on domain embeddings	11
D.2. Empirical analysis on domain amplifier	11
D.3. Comparison of number of learnable parameters	11
E Discussion	11
E.1. Statistical Analysis of Performance Improve- ments	11
E.2. Memory efficiency in storing domain embed- dings	12
E.3. Failure cases of DiCoTTA	12
F. Detailed performance	12
F.1. Detailed performance on CIFAR100-C	12
F.2. Detailed performance on ImageNet-C	13
F.3. Detailed Performance on ACDC	13

This supplementary material presents additional experimental details and results that are omitted from the main

paper due to the space limit. First, we provide the detailed algorithm of DiCoTTA in Sec. A, and the experimental details in Sec. B, including implementation details and structure of the domain amplifier. Sec. C contains an extensive ablation study to analyze the importance of DiCoTTA. Sec. D provides a comprehensive empirical analysis, and Sec. E presents the discussion of the significance of DiCoTTA. Detailed performance on CIFAR100-C, ImageNet-C, and ACDC is reported in Sec. F. Finally, instructions on running the source code and test logs are provided in Sec. ??.

A. Algorithm of DiCoTTA

Algorithm 1 outlines the test-time adaptation procedure of DiCoTTA.

Algorithm 1 CTTA Algorithm of DiCoTTA

Input: Pre-trained encoder ϕ_{enc} , classification head ψ_{cls} , domain information extractor ψ_{domain} , domain amplifier ψ_{amp} , batch size n , test data stream $X = \{x_i\}_{i=1}^n$, previous domain prototypes \mathcal{P}_{pre} , previous domain embedding queue \mathcal{Q}_{pre}

- 1: **for** each batch $X_i = \{x_j\}_{j=1}^n$ in test data stream **do**
- 2: Obtain predictions $\hat{Y}_i = \{\psi_{\text{cls}}(\phi_{\text{enc}}(x_j)) \mid x_j \in X_i\}$
- 3: Compute prediction confidence score c_i
- 4: **if** $|c_i - c_{i-1}| > \tau$ **then** // Detect domain change
- 5: $\mathcal{P}_{\text{pre}} \leftarrow \text{SELECTPROTOTYPES}(\mathcal{Q}_{\text{pre}}, \psi_{\text{domain}})$
- 6: $\mathcal{Q}_{\text{pre}} \leftarrow \emptyset$ // Reset previous queue
- 7: **end if**
- 8: $\mathcal{F}_{\text{cur}} \leftarrow \emptyset$
- 9: **Stage 1: Extract domain embeddings**
- 10: **for** each sample x_j in X_i **do**
- 11: $f_j = \psi_{\text{domain}}(\phi_{\text{enc}} + \psi_{\text{amp}})(x_j)$ // Compute domain embeddings
- 12: $\mathcal{F}_{\text{cur}} \leftarrow \mathcal{F}_{\text{cur}} \cup \{f_j\}$
- 13: **end for**
- 14: Freeze ϕ_{enc} and ψ_{cls}
- 15: $\mathcal{L}_{\text{dis}} \leftarrow \mathcal{L}_{\text{dis}}(\mathcal{F}_{\text{cur}}, \mathcal{P}_{\text{pre}})$
- 16: $\mathcal{L}_{\text{self}} \leftarrow \mathcal{L}_{\text{self}}(\hat{Y}_i)$
- 17: Update ψ_{domain} and ψ_{amp}
- 18: **Stage 2: Learning domain-invariant features**
- 19: Freeze ψ_{amp} and ψ_{domain}
- 20: $\mathcal{L}_{\text{self}} \leftarrow \mathcal{L}_{\text{self}}(\hat{Y}_i)$
- 21: $\mathcal{L}_{\text{inv}} \leftarrow \mathcal{L}_{\text{inv}}(\mathcal{F}_{\text{cur}}, \mathcal{P}_{\text{pre}})$
- 22: Update ϕ_{enc} and ψ_{cls}
- 23: **Update domain prototypes**
- 24: $\mathcal{L}_{\text{update}} \leftarrow \mathcal{L}_{\text{update}}(\mathcal{F}_{\text{cur}}, \mathcal{P}_{\text{pre}})$
- 25: Update \mathcal{P}_{pre}
- 26: Enqueue all domain embeddings $f_j \in \mathcal{F}_{\text{cur}}$ into \mathcal{Q}_{pre}
- 27: **end for**

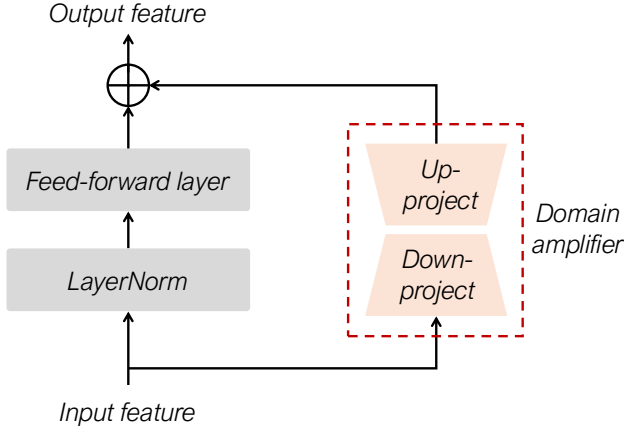


Figure a1. Domain amplifier structure. The domain amplifier is attached to each layer of the encoder, consisting of a down-projection layer followed by an up-projection layer.

B. Experimental details

B.1. Implementation details

We employ a single A6000 GPU for classification tasks (*e.g.*, CIFAR10-C, CIFAR100-C, ImageNet-C) and a TITAN RTX GPU for semantic segmentation (*e.g.*, ACDC). Following previous work [44], the batch sizes are set to $\{40, 50, 50, 1\}$ for $\{\text{CIFAR10-C, CIFAR100-C, ImageNet-C, ACDC}\}$, respectively. The learning rates of the encoder are $\{1e-4, 3e-4, 5e-7, 2e-3\}$, and the optimizers are $\{\text{Adam, Adam, SGD, AdamW}\}$, respectively. The learning rates of the amplifier are $\{6e-5, 9e-6, 2e-7, 2e-3\}$, and the optimizers are $\{\text{Adam, Adam, SGD, AdamW}\}$, respectively. We store up to 256 domain embeddings in a queue (512 for CIFAR100-C and ImageNet-C) and keep domain prototypes the same with each batch size. Following prior CTTA works [17, 44, 62], we pre-train *only* our domain amplifier module on the source dataset for 5 epochs. The same optimizer and learning rate as used at test time are also employed in this pre-training step.

B.2. Structure of domain amplifier

Fig. a1 illustrates how the domain amplifier is integrated into each layer of the encoder. Following the conventional adapter structure for parameter-efficient fine-tuning [10, 27, 55], the domain amplifier uses a bottleneck structure (down-projection, then up-projection) to capture domain-specific information while keeping parameter overhead minimal. Attaching a domain amplifier to each encoder layer allows the model to incorporate domain cues at multiple semantic levels, facilitating robust adaptation in non-stationary test settings.

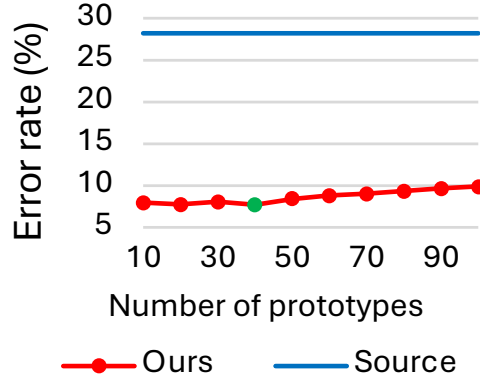


Figure a2. Ablation study on the number of domain prototypes.

Metric	MMD	Hausdorff	Chamfer
Error	8.2	8.1	7.7

Table a1. Ablation study on distance metrics used in prototype update

C. Additional ablation study

C.1. Ablation study on number of domain prototypes

We conduct an ablation study on the number of domain prototypes to analyze its impact on DiCoTTA’s performance. As shown in Fig. a2, we vary the number of domain prototypes from 10 to 100 while keeping other hyperparameters fixed. The results show that having too few prototypes leads to degraded performance as they cannot sufficiently capture the domain characteristics. However, using too many prototypes not only increases computational overhead but also risks including outliers. We find that DiCoTTA is insensitive to the number of domain prototypes while maintaining a good balance between memory consumption and representation capability.

C.2. Ablation study on distance metrics for prototype update

We investigate the effectiveness of different distance metrics (*i.e.*, MMD, Hausdorff, and Chamfer) for updating the prototypes in the domain embedding space. As Chamfer distance is sensitive to individual point shifts, it more effectively ensures that each prototype remains consistent in the domain embedding space before and after model updates. Consequently, as shown in Table a1, using Chamfer distance results in the lowest error among the three metrics, demonstrating its suitability for prototype updates.

Length	8192	16384	32768	Conf	0.4	0.6	0.8
Error	8.1	8.0	8.1	Error	8.1	8.3	8.1

(a) Effect of queue length (b) Effect of confidence threshold

Table a2. Ablation study on queue length $|\mathcal{F}_{\text{pre}}|$ and confidence threshold for domain change detection.

C.3. Extended ablation study on thresholds

We expand the ablation studies of Fig. 6 in the main paper to include a wider range of queue lengths and domain change detection thresholds. The results below show that DiCoTTA remains robust to a very wide range of thresholds.

D. Empirical analysis

D.1. Empirical analysis on domain embeddings

To better understand how DiCoTTA learns domain-specific features, *i.e.* domain embeddings, we analyze the domain embeddings before and after Stage 1 (domain-specific learning). Figure a3(a) shows the t-SNE visualization of domain embeddings from different domains, where each color represents a different domain. Before Stage 1, the domain embeddings are scattered without clear domain-wise clustering. However, after Stage 1, we observe distinct domain-wise clusters, indicating that our domain embeddings effectively capture domain-specific characteristics. We further quantitatively analyze the domain gap using Chamfer distance between domain embeddings from different domains, as shown in Figure a3(b). The increased Chamfer distance after Stage 1 confirms that our domain-specific learning successfully extracts domain-specific features in terms of domain embeddings.

D.2. Empirical analysis on domain amplifier

In the main text, we analyzed how the domain amplifier influences attention heatmaps under domain-invariant learning in Fig. 5 of the main paper. Here, we present further examples (Fig. a4) illustrating that enabling the domain amplifier consistently yields more reliable attention maps across varied domains, even under challenging environmental shifts. Fig. a4 revealed that enabling the domain amplifier produces more reliable attention maps across diverse domains, even under varying environmental shifts.

D.3. Comparison of number of learnable parameters

We compare the number of learnable parameters between DiCoTTA and other CTTA methods in Table a4. As shown in the table, DiCoTTA requires only 7.0M additional parameters compared to TENT and CoTTA, which is a modest increase considering the significant performance improvement. Despite having more parameters than some baselines,

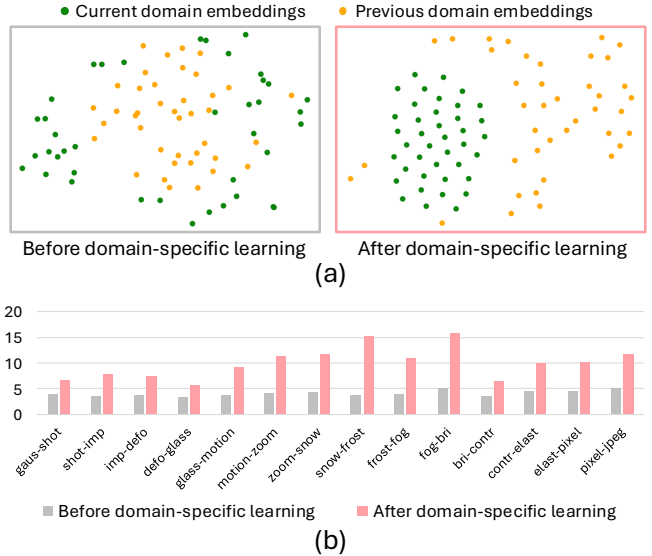


Figure a3. Empirical analysis on the impact of domain embeddings in DiCoTTA. (a) 2D visualization of the distribution of domain embeddings from different domains before and after Stage 1, *i.e.*, domain-specific learning. (b) The domain gap between different domains is measured by Chamfer distance before and after applying domain-specific learning.

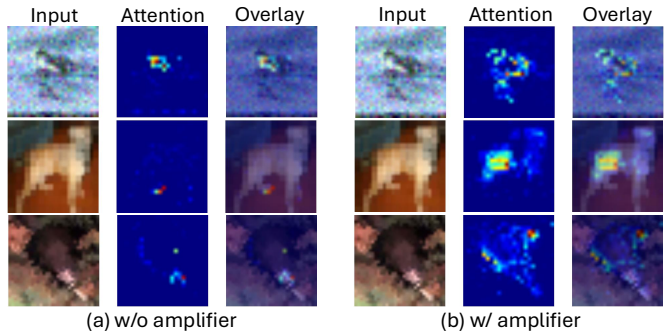


Figure a4. Empirical analysis on the impact of the domain amplifier. (a) Without amplifier (b) With amplifier

DiCoTTA achieves substantially better performance, demonstrating that the additional parameters are used effectively to capture domain-specific features and enhance adaptation.

E. Discussion

E.1. Statistical Analysis of Performance Improvements

To rigorously evaluate the effectiveness of our method, we perform statistical significance testing by conducting paired t-tests between DiCoTTA and existing methods on the ACDC dataset. The results in Table a5 demonstrate that our improvements are statistically significant, with all p-values falling well below the standard significance level of 0.05.

Method	gaussian	shot	impulse	defocus	glass	motion	zoom	snow	frost	fog	brightness	contrast	elastic_trans	pixelate	jpeg	Mean↓	Gain
Source [13] ICLR2021	55.0	51.5	26.9	24.0	60.5	29.0	21.4	21.1	25.0	35.2	11.8	34.8	43.2	56.0	35.9	35.4	/
Pseudo [36] ICML2013	53.8	48.9	25.4	23.0	58.7	27.3	19.6	20.6	23.4	31.3	11.8	28.4	39.6	52.3	33.9	33.2	+2.2
TENT [68] ICLR2021	53.0	47.0	24.6	22.3	58.5	26.5	19.0	21.0	23.0	30.1	11.8	25.2	39.0	47.1	33.3	32.1	+3.3
CoTTA [71] CVPR2022	55.0	51.3	25.8	24.1	59.2	28.9	21.4	21.0	24.7	34.9	11.7	31.7	40.4	55.7	35.6	34.8	+0.6
VDP [17] AAAI2023	54.8	51.2	25.6	24.2	59.1	28.8	21.2	20.5	23.3	33.8	7.5	11.7	32.0	51.7	35.2	32.0	+3.4
ViDA [44] ICLR2024	50.1	40.7	22.0	21.2	45.2	21.6	16.5	17.9	16.6	25.6	11.5	29.0	29.6	34.7	27.1	27.3	+8.1
Continual-MAE [43] CVPR2024	48.6	30.7	18.5	21.3	38.4	22.2	17.5	19.3	18.0	24.8	13.1	27.8	31.4	35.5	29.5	26.4	+9.0
Yang <i>et al.</i> [75] CVPR2024	38.2	31.8	18.2	20.8	34.3	20.3	17.5	14.9	16.2	22.9	11.5	27.5	28.2	32.5	25.3	24.0	+11.4
DiCoTTA	40.7	32.8	21.0	21.7	36.9	20.8	16.5	17.5	15.7	22.7	12.9	22.5	22.4	20.6	24.3	23.3	+12.1

Table a3. Fine-grained classification error rates (%) on CIFAR100-to-CIFAR100-C online CTTA task. Gain (%) represents the percentage of improvement in accuracy compared with the source method.

Method	Error rate (%)	Parameters
TENT [68]	23.5	86.1M
CoTTA [71]	24.6	86.1M
ViDA [44]	20.7	93.2M
Continual-MAE [43]	12.6	86.1M
DiCoTTA (Ours)	7.7	93.1M

Table a4. Comparison of error rates and number of learnable parameters across different CTTA methods.

Dataset	p-value
Source [73] ICLR2021 vs. Ours	6.77×10^{-8}
TENT [69] ICLR2021 vs. Ours	3.51×10^{-8}
CoTTA [71] CVPR2022 vs. Ours	3.55×10^{-7}
DePT [19] arXiv vs. Ours	1.06×10^{-8}
ECoTTA [62] CVPR2023 vs. Ours	3.73×10^{-8}
VDP [17] AAAI2023 vs. Ours	2.60×10^{-7}
ViDA [44] ICLR2024 vs. Ours	2.30×10^{-3}
BECoTTA [35] ICML2024 vs. Ours	1.08×10^{-6}
SVDP [74] AAAI2024 vs. Ours	6.52×10^{-5}
Continual-MAE [43] CVPR2024 vs. Ours	9.80×10^{-4}
Zhu <i>et al.</i> [82] ECCV2024 vs. Ours	2.30×10^{-5}

Table a5. Statistical significance test results (p-values) comparing DiCoTTA with existing methods on ACDC. All p-values are less than 0.05, indicating that our improvements are statistically significant.

The obtained p-values, ranging from 10^{-8} to 10^{-3} , strongly support that DiCoTTA achieves meaningful performance gains over existing methods in continual test-time adaptation rather than improvements due to random variation.

E.2. Memory efficiency in storing domain embeddings

Our method achieves efficient memory utilization through a selective domain embedding storage strategy. Rather than storing embeddings from all encountered domains, we maintain only 40 domain prototypes from the immediately previous domain and 256 domain embeddings from the current domain. This focused approach results in a minimal memory overhead of just 0.4MB while preserving the model’s ability to effectively handle domain shifts. Our experimental analysis, as shown in Fig. 6 of the main paper, demonstrates that we can further optimize memory usage by reducing the domain queue length to 64 without compromising prediction accuracy. This memory-efficient design enables our approach to achieve state-of-the-art performance while remaining practical for real-world applications with limited computational resources.

E.3. Failure cases of DiCoTTA

Fig. a5 illustrates the failure cases of DiCoTTA on CIFAR10-C. In CTTA, since only a limited number of test samples are accessible per iteration, the model lacks sufficient exposure to diverse domain shifts at the beginning, making it less robust to initial corruptions such as noise and blur. Additionally, when encountering extremely corrupted scenes, the model is hard to maintain robustness, leading to performance degradation.

F. Detailed performance

F.1. Detailed performance on CIFAR100-C

Table a3 shows the detailed performance of DiCoTTA and other CTTA methods on CIFAR100-to-CIFAR100-C task. DiCoTTA achieves the best overall performance with a 23.3% error rate, showing a 12.1% improvement over the source model. Notably, DiCoTTA performs particularly well on challenging corruptions like pixelate (20.6%) and elastic transform (22.4%), outperforming other methods by signifi-

Method	<i>gaussian</i>	<i>shot</i>	<i>impulse</i>	<i>defocus</i>	<i>glass</i>	<i>motion</i>	<i>zoom</i>	<i>snow</i>	<i>frost</i>	<i>fog</i>	<i>brightness</i>	<i>contrast</i>	<i>elastic_trans</i>	<i>pixelate</i>	<i>jpeg</i>	Mean↓	Gain
Source [13] ICLR2021	53.0	51.8	52.1	68.5	78.8	58.5	63.3	49.9	54.2	57.7	26.4	91.4	57.5	38.0	36.2	55.8	/
Pseudo [36] ICML2013	45.2	40.4	41.6	51.3	53.9	45.6	47.7	40.4	45.7	93.8	98.5	99.9	99.9	98.9	99.6	61.2	-5.4
TENT [68] ICLR2021	52.2	48.9	49.2	65.8	73.0	54.5	58.4	44.0	47.7	50.3	23.9	72.8	55.7	34.4	33.9	51.0	+4.8
CoTTA [71] CVPR2022	52.9	51.6	51.4	68.3	78.1	57.1	62.0	48.2	52.7	55.3	25.9	90.0	56.4	36.4	35.2	54.8	+1.0
VDP [17] AAAI2023	52.7	51.6	50.1	58.1	70.2	56.1	58.1	42.1	46.1	45.8	23.6	70.4	54.9	34.5	36.1	50.0	+5.8
ViDA [44] ICLR2024	47.7	42.5	42.9	52.2	56.9	45.5	48.9	38.9	42.7	40.7	24.3	52.8	49.1	33.5	33.1	43.4	+12.4
Continual-MAE [43] CVPR2024	46.3	41.9	42.5	51.4	54.9	43.3	40.7	34.2	35.8	64.3	23.4	60.3	37.5	29.2	31.4	42.5	+13.3
Yang <i>et al.</i> [75]	47.5	42.1	41.6	55.5	55.4	44.5	47.9	38.8	37.8	39.6	23.6	57.0	44.4	33.5	32.3	42.7	+13.1
DiCoTTA	46.5	41.8	41.8	47.7	57.3	44.0	49.1	39.7	42.4	39.3	23.7	49.7	50.5	32.2	32.4	42.5	+13.3

Table a6. Fine-grained classification error rates (%) on ImageNet-to-ImageNet-C online CTTA task. Gain (%) represents the percentage of improvement in accuracy compared with the source method.

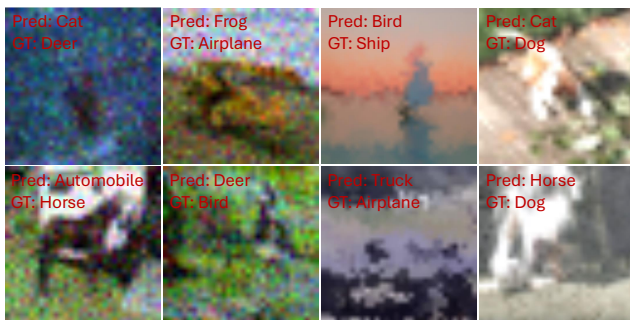


Figure a5. Failure cases of DiCoTTA.

cant margins. This demonstrates DiCoTTA’s effectiveness in handling diverse types of corruptions in fine-grained classification tasks.

F.2. Detailed performance on ImageNet-C

Table a6 shows the detailed performance of DiCoTTA and other CTTA methods on ImageNet-to-ImageNet-C task. DiCoTTA achieves competitive performance with a 42.5% error rate, showing a 13.3% improvement over the source model. DiCoTTA performs particularly well on challenging corruptions like defocus blur (47.7%) and contrast (49.7%), demonstrating its effectiveness in handling diverse types of corruptions in large-scale classification tasks.

F.3. Detailed Performance on ACDC

Table a7 presents the CTTA results of DiCoTTA on the Cityscapes-to-ACDC. We report the results from two independent trials to assess the consistency and robustness of our method. Across all trials, DiCoTTA consistently achieves superior performance compared to existing CTTA methods. This stability across multiple trials highlights the effectiveness of our approach in handling domain shifts.

Time	$t \longrightarrow$															
Round	1					2					3					Mean \uparrow
Method	Fog	Night	Rain	Snow	Mean \uparrow	Fog	Night	Rain	Snow	Mean \uparrow	Fog	Night	Rain	Snow	Mean \uparrow	Mean \uparrow
Source [73] ICLR2021	69.1	40.3	59.7	57.8	56.7	69.1	40.3	59.7	57.8	56.7	69.1	40.3	59.7	57.8	56.7	56.7
TENT [69] ICLR2021	69.0	40.2	60.1	57.3	56.7	68.3	39.0	60.1	56.3	55.9	67.5	37.8	59.6	55.0	55.0	55.7
CoTTA [71] CVPR2022	70.9	41.2	62.4	59.7	58.6	70.9	41.1	62.6	59.7	58.6	70.9	41.0	62.7	59.7	58.6	58.6
DePT [19] arXiv	71.0	40.8	58.2	56.8	56.5	68.2	40.0	55.4	53.7	54.3	66.4	38.0	47.3	47.2	49.7	53.4
ECoTTA [62] CVPR2023	68.5	35.8	62.1	57.4	56.0	68.3	35.5	62.3	57.4	55.9	68.1	35.3	62.3	57.3	55.8	55.8
VDP [17] AAAI2023	70.5	41.1	62.1	59.5	58.3	70.4	41.1	62.2	59.4	58.2	70.4	41.0	62.2	59.4	58.2	58.2
ViDA [44] ICLR2024	71.6	43.2	66.0	63.4	61.1	73.2	44.5	67.0	63.9	62.2	73.2	44.6	67.2	64.2	62.3	61.9
BECoTTA [35] ICML2024	72.3	42.0	63.5	60.1	59.5	72.4	41.9	63.5	60.2	59.5	72.3	41.9	63.6	60.2	59.5	59.5
SVDP [74] AAAI2024	72.1	44.0	65.2	63.0	61.1	72.2	44.5	65.9	63.5	61.5	72.1	44.2	65.6	63.6	61.4	61.3
Continual-MAE [43] CVPR2024	71.9	44.6	67.4	63.2	61.8	71.7	44.9	66.5	63.1	61.6	72.3	45.4	67.1	63.1	62.0	61.8
Zhu <i>et al.</i> [82] ECCV2024	71.2	42.3	64.9	62.0	60.1	72.6	43.2	66.3	63.2	61.3	72.8	43.8	66.5	63.2	61.6	61.0
DiCoTTA-trial1	71.9	45.2	66.6	64.1	62.0	73.3	45.7	67.8	64.1	62.7	73.0	44.4	67.9	63.7	62.3	62.3
DiCoTTA-trial2	71.8	45.8	66.2	63.6	61.9	73.0	45.9	67.0	64.0	62.5	72.5	44.9	67.9	63.6	62.2	62.2
DiCoTTA-mean	71.9	45.5	66.4	63.9	62.0 ± 0.1	73.2	45.8	67.4	64.1	62.6 ± 0.1	72.8	44.7	67.9	63.7	62.3 ± 0.1	62.3 ± 0.1

Table a7. Segmentation results on Cityscape-to-ACDC online CTTA task. We report results from two independent trials, where the final mean mIoU is computed with standard deviation.

References

- [1] Abien Fred Agarap. Deep learning using rectified linear units (relu). *arXiv preprint arXiv:1803.08375*, 2018. 6
- [2] Nader Asadi, MohammadReza Davari, Sudhir Mudur, Rahaf Aljundi, and Eugene Belilovsky. Prototype-sample relation distillation: towards replay-free continual learning. In *Proc. International Conference on Machine Learning (ICML)*, 2023. 5
- [3] Yogesh Balaji, Swami Sankaranarayanan, and Rama Chellappa. Metareg: Towards domain generalization using meta-regularization. *Advances in neural information processing systems*, 31, 2018. 2
- [4] David Brüggenmann, Christos Sakaridis, Tim Brödermann, and Luc Van Gool. Contrastive model adaptation for cross-condition robustness in semantic segmentation. In *Proc. IEEE/CVF International Conference on Computer Vision (ICCV)*, 2023. 1
- [5] Zhaowei Cai and Nuno Vasconcelos. Cascade r-cnn: Delving into high quality object detection. In *Proc. IEEE/CVF Conference on Computer Vision and Pattern Recognition (CVPR)*, 2018. 1
- [6] Nicolas Carion, Francisco Massa, Gabriel Synnaeve, Nicolas Usunier, Alexander Kirillov, and Sergey Zagoruyko. End-to-end object detection with transformers. In *European conference on computer vision*, pages 213–229. Springer, 2020. 1
- [7] Junbum Cha, Sanghyuk Chun, Kyungjae Lee, Han-Cheol Cho, Seunghyun Park, Yunsung Lee, and Sungrae Park. Swad: Domain generalization by seeking flat minima. *Advances in Neural Information Processing Systems*, 34:22405–22418, 2021. 2
- [8] Woong-Gi Chang, Tackgeun You, Seonguk Seo, Suha Kwak, and Bohyung Han. Domain-specific batch normalization for unsupervised domain adaptation. In *Proc. IEEE/CVF Conference on Computer Vision and Pattern Recognition (CVPR)*, 2019. 1
- [9] Liang-Chieh Chen, Yukun Zhu, George Papandreou, Florian Schroff, and Hartwig Adam. Encoder-decoder with atrous separable convolution for semantic image segmentation. In *Proc. European Conference on Computer Vision (ECCV)*, 2018. 1
- [10] Shoufa Chen, Chongjian Ge, Zhan Tong, Jiangliu Wang, Yibing Song, Jue Wang, and Ping Luo. Adaptformer: Adapting vision transformers for scalable visual recognition. In *Proc. Neural Information Processing Systems (NeurIPS)*, 2022. 3, 10
- [11] Marius Cordts, Mohamed Omran, Sebastian Ramos, Timo Rehfeld, Markus Enzweiler, Rodrigo Benenson, Uwe Franke, Stefan Roth, and Bernt Schiele. The cityscapes dataset for semantic urban scene understanding. In *Proc. IEEE/CVF Conference on Computer Vision and Pattern Recognition (CVPR)*, 2016. 2, 6
- [12] Jia Deng, Wei Dong, Richard Socher, Li-Jia Li, Kai Li, and Li Fei-Fei. ImageNet: a large-scale hierarchical image database. In *Proc. IEEE/CVF Conference on Computer Vision and Pattern Recognition (CVPR)*, 2009. 2
- [13] Alexey Dosovitskiy, Lucas Beyer, Alexander Kolesnikov, Dirk Weissenborn, Xiaohua Zhai, Thomas Unterthiner, Mostafa Dehghani, Matthias Minderer, Georg Heigold, Sylvain Gelly, et al. An image is worth 16x16 words: Transformers for image recognition at scale. In *Proc. International Conference on Learning Representations (ICLR)*, 2021. 1, 6, 7, 12, 13
- [14] Qi Dou, Daniel Coelho de Castro, Konstantinos Kamnitsas, and Ben Glocker. Domain generalization via model-agnostic learning of semantic features. *Advances in neural information processing systems*, 32, 2019. 2
- [15] Cian Eastwood, Ian Mason, Christopher KI Williams, and Bernhard Schölkopf. Source-free adaptation to measurement shift via bottom-up feature restoration. *arXiv preprint arXiv:2107.05446*, 2021. 2
- [16] Pierre Foret, Ariel Kleiner, Hossein Mobahi, and Behnam Neyshabur. Sharpness-aware minimization for efficiently improving generalization. *arXiv preprint arXiv:2010.01412*, 2020. 2
- [17] Yulu Gan, Yan Bai, Yihang Lou, Xianzheng Ma, Renrui Zhang, Nian Shi, and Lin Luo. Decorate the newcomers: Visual domain prompt for continual test time adaptation. In *Proceedings of the AAAI Conference on Artificial Intelligence*, pages 7595–7603, 2023. 1, 2, 3, 4, 6, 7, 8, 10, 12, 13, 14
- [18] Yaroslav Ganin and Victor Lempitsky. Unsupervised domain adaptation by backpropagation. In *Proc. International Conference on Machine Learning (ICML)*, 2015. 1, 2
- [19] Yunhe Gao, Xingjian Shi, Yi Zhu, Hao Wang, Zhiqiang Tang, Xiong Zhou, Mu Li, and Dimitris N Metaxas. Visual prompt tuning for test-time domain adaptation. *arXiv preprint arXiv:2210.04831*, 2022. 8, 12, 14
- [20] Ross Girshick, Jeff Donahue, Trevor Darrell, and Jitendra Malik. Rich feature hierarchies for accurate object detection and semantic segmentation. In *Proc. IEEE/CVF Conference on Computer Vision and Pattern Recognition (CVPR)*, 2014. 1
- [21] Ian Goodfellow, Jean Pouget-Abadie, Mehdi Mirza, Bing Xu, David Warde-Farley, Sherjil Ozair, Aaron Courville, and Yoshua Bengio. Generative adversarial networks. *Communications of the ACM*, 63(11):139–144, 2020. 2
- [22] Chuan Guo, Geoff Pleiss, Yu Sun, and Kilian Q Weinberger. On calibration of modern neural networks. In *Proc. International Conference on Machine Learning (ICML)*, 2017. 1
- [23] Sivan Harary, Eli Schwartz, Assaf Arbelle, Peter Staar, Shady Abu-Hussein, Elad Amrani, Roi Herzig, Amit Alfassy, Raja Giryes, Hilde Kuehne, et al. Unsupervised domain generalization by learning a bridge across domains. In *Proceedings of the IEEE/CVF Conference on Computer Vision and Pattern Recognition*, pages 5280–5290, 2022. 2
- [24] Kaiming He, Xiangyu Zhang, Shaoqing Ren, and Jian Sun. Deep residual learning for image recognition. In *Proc. IEEE/CVF Conference on Computer Vision and Pattern Recognition (CVPR)*, 2016. 1
- [25] Dan Hendrycks and Thomas Dietterich. Benchmarking neural network robustness to common corruptions and perturbations. In *Proc. International Conference on Learning Representations (ICLR)*, 2019. 1, 2, 6

- [26] Dan Hendrycks and Kevin Gimpel. Gaussian error linear units (gelus). *arXiv preprint arXiv:1606.08415*, 2016. 6
- [27] Neil Houlsby, Andrei Giurgiu, Stanislaw Jastrzebski, Bruna Morrone, Quentin De Laroussilhe, Andrea Gesmundo, Mona Attariyan, and Sylvain Gelly. Parameter-efficient transfer learning for nlp. In *Proc. International Conference on Machine Learning (ICML)*. PMLR, 2019. 3, 10
- [28] Yunpei Jia, Jie Zhang, Shiguang Shan, and Xilin Chen. Single-side domain generalization for face anti-spoofing. In *Proc. IEEE/CVF Conference on Computer Vision and Pattern Recognition (CVPR)*, 2020. 2
- [29] Juwon Kang, Sohyun Lee, Namyup Kim, and Suha Kwak. Style neophile: Constantly seeking novel styles for domain generalization. In *Proceedings of the IEEE/CVF Conference on Computer Vision and Pattern Recognition*, pages 7130–7140, 2022. 2
- [30] Juwon Kang, Nayeong Kim, Donghyeon Kwon, Jungseul Ok, and Suha Kwak. Leveraging proxy of training data for test-time adaptation. In *Proc. International Conference on Machine Learning (ICML)*, 2023. 1, 2
- [31] Juwon Kang, Nayeong Kim, Jungseul Ok, and Suha Kwak. Membn: Robust test-time adaptation via batch norm with statistics memory. In *Proc. European Conference on Computer Vision (ECCV)*, 2024. 1
- [32] Been Kim, Rajiv Khanna, and Oluwasanmi O Koyejo. Examples are not enough, learn to criticize! criticism for interperability. In *Proc. Neural Information Processing Systems (NeurIPS)*, 2016. 2, 4
- [33] Alexander Kirillov, Eric Mintun, Nikhila Ravi, Hanzi Mao, Chloe Rolland, Laura Gustafson, Tete Xiao, Spencer Whitehead, Alexander C Berg, Wan-Yen Lo, et al. Segment anything. In *Proceedings of the IEEE/CVF International Conference on Computer Vision*, pages 4015–4026, 2023. 7
- [34] Alex Krizhevsky, Geoffrey Hinton, et al. Learning multiple layers of features from tiny images. 2009. 2
- [35] Daeun Lee, Jaehong Yoon, and Sung Ju Hwang. Becotta: Input-dependent online blending of experts for continual test-time adaptation. In *Proc. International Conference on Machine Learning (ICML)*, 2024. 1, 2, 8, 12, 14
- [36] Dong-Hyun Lee et al. Pseudo-label: The simple and efficient semi-supervised learning method for deep neural networks. In *Workshop on challenges in representation learning, ICML*, page 896. Atlanta, 2013. 6, 7, 12, 13
- [37] Sohyun Lee, Taeyoung Son, and Suha Kwak. Fifo: Learning fog-invariant features for foggy scene segmentation. In *Proc. IEEE/CVF Conference on Computer Vision and Pattern Recognition (CVPR)*, 2022. 1, 4
- [38] Sohyun Lee, Namyup Kim, Sungyeon Kim, and Suha Kwak. Frest: Feature restoration for semantic segmentation under multiple adverse conditions. In *Proc. European Conference on Computer Vision (ECCV)*, 2024. 1
- [39] Da Li, Yongxin Yang, Yi-Zhe Song, and Timothy M Hospedales. Deeper, broader and artier domain generalization. In *Proc. IEEE/CVF International Conference on Computer Vision (ICCV)*, 2017. 6
- [40] Shuang Li, Chi Liu, Qiuxia Lin, Binhui Xie, Zhengming Ding, Gao Huang, and Jian Tang. Domain conditioned adaptation network. In *Proc. AAAI Conference on Artificial Intelligence (AAAI)*, 2020. 2
- [41] Xiang Li, Wenhai Wang, Xiaolin Hu, and Jian Yang. Selective kernel networks. In *Proc. IEEE/CVF Conference on Computer Vision and Pattern Recognition (CVPR)*, 2019. 1
- [42] Ya Li, Xinmei Tian, Mingming Gong, Yajing Liu, Tongliang Liu, Kun Zhang, and Dacheng Tao. Deep domain generalization via conditional invariant adversarial networks. In *Proc. European Conference on Computer Vision (ECCV)*, 2018. 2
- [43] Jiaming Liu, Ran Xu, Senqiao Yang, Renrui Zhang, Qizhe Zhang, Zehui Chen, Yandong Guo, and Shanghang Zhang. Continual-mae: Adaptive distribution masked autoencoders for continual test-time adaptation. In *Proc. IEEE/CVF Conference on Computer Vision and Pattern Recognition (CVPR)*, 2024. 1, 2, 6, 7, 8, 12, 13, 14
- [44] Jiaming Liu, Senqiao Yang, Peidong Jia, Ming Lu, Yandong Guo, Wei Xue, and Shanghang Zhang. Vida: Homeostatic visual domain adapter for continual test time adaptation. In *Proc. International Conference on Learning Representations (ICLR)*, 2024. 1, 2, 4, 6, 7, 8, 10, 12, 13, 14
- [45] Pengfei Liu, Weizhe Yuan, Jinlan Fu, Zhengbao Jiang, Hiroaki Hayashi, and Graham Neubig. Pre-train, prompt, and predict: A systematic survey of prompting methods in natural language processing. *ACM Computing Surveys*, 55(9):1–35, 2023. 7
- [46] Yuejiang Liu, Parth Kothari, Bastien van Delft, Baptiste Bellot-Gurlet, Taylor Mordan, and Alexandre Alahi. Ttt++: When does self-supervised test-time training fail or thrive? In *Proc. Neural Information Processing Systems (NeurIPS)*, 2021. 2
- [47] Yair Movshovitz-Attias, Alexander Toshev, Thomas K Leung, Sergey Ioffe, and Saurabh Singh. No fuss distance metric learning using proxies. In *Proc. IEEE/CVF International Conference on Computer Vision (ICCV)*, 2017. 4
- [48] Chaithanya Kumar Mummadi, Robin Huttmacher, Kilian Ram-bach, Evgeny Levinkov, Thomas Brox, and Jan Hendrik Metzen. Test-time adaptation to distribution shift by confidence maximization and input transformation. *arXiv preprint arXiv:2106.14999*, 2021. 1
- [49] Hyeonseob Nam, HyunJae Lee, Jongchan Park, Wonjun Yoon, and Donggeun Yoo. Reducing domain gap by reducing style bias. In *Proceedings of the IEEE/CVF Conference on Computer Vision and Pattern Recognition*, pages 8690–8699, 2021. 2
- [50] George L Nemhauser, Laurence A Wolsey, and Marshall L Fisher. An analysis of approximations for maximizing submodular set functions—i. *Mathematical programming*, 14(1): 265–294, 1978. 2, 4
- [51] Shuaicheng Niu, Jiayang Wu, Yifan Zhang, Yaofu Chen, Shijian Zheng, Peilin Zhao, and Mingkui Tan. Efficient test-time model adaptation without forgetting. In *International conference on machine learning*, pages 16888–16905. PMLR, 2022. 1, 2
- [52] Shuaicheng Niu, Jiayang Wu, Yifan Zhang, Zhiquan Wen, Yaofu Chen, Peilin Zhao, and Mingkui Tan. Towards stable test-time adaptation in dynamic wild world. *arXiv preprint arXiv:2302.12400*, 2023. 1, 2

- [53] Hyeonwoo Noh, Seunghoon Hong, and Bohyung Han. Learning deconvolution network for semantic segmentation. In *Proc. IEEE/CVF International Conference on Computer Vision (ICCV)*, 2015. 1
- [54] Maxime Oquab, Timothée Darcet, Théo Moutakanni, Huy Vo, Marc Szafraniec, Vasil Khalidov, Pierre Fernandez, Daniel Haziza, Francisco Massa, Alaaeldin El-Nouby, et al. Dinov2: Learning robust visual features without supervision. *arXiv preprint arXiv:2304.07193*, 2023. 7
- [55] Jonas Pfeiffer, Aishwarya Kamath, Andreas Rücklé, Kyunghyun Cho, and Iryna Gurevych. Adapterfusion: Non-destructive task composition for transfer learning. *arXiv preprint arXiv:2005.00247*, 2020. 3, 10
- [56] Aditya Ramesh, Prafulla Dhariwal, Alex Nichol, Casey Chu, and Mark Chen. Hierarchical text-conditional image generation with clip latents. *arXiv preprint arXiv:2204.06125*, 2022. 7
- [57] Christos Sakaridis, Dengxin Dai, Simon Hecker, and Luc Van Gool. Model adaptation with synthetic and real data for semantic dense foggy scene understanding. In *Proc. European Conference on Computer Vision (ECCV)*, 2018. 1
- [58] Christos Sakaridis, Dengxin Dai, and Luc Van Gool. Semantic foggy scene understanding with synthetic data. *International Journal of Computer Vision (IJCV)*, 2018.
- [59] Christos Sakaridis, Dengxin Dai, and Luc Van Gool. Guided curriculum model adaptation and uncertainty-aware evaluation for semantic nighttime image segmentation. In *Proc. IEEE/CVF International Conference on Computer Vision (ICCV)*, 2019. 1
- [60] Christos Sakaridis, Dengxin Dai, and Luc Van Gool. ACDC: The adverse conditions dataset with correspondences for semantic driving scene understanding. In *Proc. IEEE/CVF International Conference on Computer Vision (ICCV)*, 2021. 2, 6
- [61] Rui Shao, Xiangyuan Lan, Jiawei Li, and Pong C Yuen. Multi-adversarial discriminative deep domain generalization for face presentation attack detection. In *Proc. IEEE/CVF Conference on Computer Vision and Pattern Recognition (CVPR)*, 2019. 2
- [62] Junha Song, Jungsoo Lee, In So Kweon, and Sungha Choi. Ecotta: Memory-efficient continual test-time adaptation via self-distilled regularization. In *Proceedings of the IEEE/CVF Conference on Computer Vision and Pattern Recognition*, pages 11920–11929, 2023. 1, 2, 8, 10, 12, 14
- [63] Yongyi Su, Xun Xu, and Kui Jia. Revisiting realistic test-time training: Sequential inference and adaptation by anchored clustering. *arXiv preprint arXiv:2206.02721*, 2022. 2
- [64] Baochen Sun and Kate Saenko. Deep coral: Correlation alignment for deep domain adaptation. In *Computer Vision—ECCV 2016 Workshops: Amsterdam, The Netherlands, October 8-10 and 15-16, 2016, Proceedings, Part III 14*, pages 443–450. Springer, 2016. 1
- [65] Yu Sun, Xiaolong Wang, Zhuang Liu, John Miller, Alexei Efros, and Moritz Hardt. Test-time training with self-supervision for generalization under distribution shifts. In *Proc. International Conference on Machine Learning (ICML)*, pages 9229–9248, 2020. 2
- [66] Antti Tarvainen and Harri Valpola. Mean teachers are better role models: Weight-averaged consistency targets improve semi-supervised deep learning results. *Advances in neural information processing systems*, 30, 2017. 4
- [67] L.J.P van der Maaten and G.E. Hinton. Visualizing high-dimensional data using t-sne. *Journal of Machine Learning Research (JMLR)*, 2008. 5
- [68] Dequan Wang, Evan Shelhamer, Shaoteng Liu, Bruno Olshausen, and Trevor Darrell. Tent: Fully test-time adaptation by entropy minimization. In *Proc. International Conference on Learning Representations (ICLR)*, 2021. 1, 2, 8, 12, 13
- [69] Dequan Wang, Evan Shelhamer, Shaoteng Liu, Bruno Olshausen, and Trevor Darrell. Tent: Fully test-time adaptation by entropy minimization. In *Proc. International Conference on Learning Representations (ICLR)*, 2021. 6, 7, 8, 12, 14
- [70] Pengfei Wang, Zhaoxiang Zhang, Zhen Lei, and Lei Zhang. Sharpness-aware gradient matching for domain generalization. In *Proceedings of the IEEE/CVF Conference on Computer Vision and Pattern Recognition*, pages 3769–3778, 2023. 2
- [71] Qin Wang, Olga Fink, Luc Van Gool, and Dengxin Dai. Continual test-time domain adaptation. In *Proceedings of the IEEE/CVF Conference on Computer Vision and Pattern Recognition*, pages 7201–7211, 2022. 1, 2, 4, 6, 7, 8, 12, 13, 14
- [72] Ziqi Wang, Marco Loog, and Jan van Gemert. Respecting domain relations: Hypothesis invariance for domain generalization. In *Proc. International Conference on Pattern Recognition (ICPR)*, 2021. 2
- [73] Enze Xie, Wenhai Wang, Zhiding Yu, Anima Anandkumar, Jose M Alvarez, and Ping Luo. SegFormer: Simple and efficient design for semantic segmentation with transformers. In *Proc. Neural Information Processing Systems (NeurIPS)*, 2021. 1, 6, 8, 12, 14
- [74] Senqiao Yang, Jiarui Wu, Jiaming Liu, Xiaoqi Li, Qizhe Zhang, Mingjie Pan, and Shanghang Zhang. Exploring sparse visual prompt for cross-domain semantic segmentation. In *Proc. AAAI Conference on Artificial Intelligence (AAAI)*, 2024. 1, 8, 12, 14
- [75] Xu Yang, Xuan Chen, Moqi Li, Kun Wei, and Cheng Deng. A versatile framework for continual test-time domain adaptation: Balancing discriminability and generalizability. In *Proc. IEEE/CVF Conference on Computer Vision and Pattern Recognition (CVPR)*, 2024. 1, 2, 6, 7, 12, 13
- [76] Marvin Zhang, Sergey Levine, and Chelsea Finn. Memo: Test time robustness via adaptation and augmentation. In *Proc. Neural Information Processing Systems (NeurIPS)*, pages 38629–38642, 2022. 1, 2
- [77] Hao Zhao, Yuejiang Liu, Alexandre Alahi, and Tao Lin. On pitfalls of test-time adaptation. *arXiv preprint arXiv:2306.03536*, 2023. 1, 2
- [78] Kaiyang Zhou, Yongxin Yang, Timothy Hospedales, and Tao Xiang. Deep domain-adversarial image generation for domain generalisation. In *Proc. AAAI Conference on Artificial Intelligence (AAAI)*, pages 13025–13032, 2020. 2
- [79] Kaiyang Zhou, Yongxin Yang, Timothy Hospedales, and Tao Xiang. Learning to generate novel domains for domain gener-

- alization. In *Proc. European Conference on Computer Vision (ECCV)*, pages 561–578. Springer, 2020. [2](#)
- [80] Kaiyang Zhou, Ziwei Liu, Yu Qiao, Tao Xiang, and Chen Change Loy. Domain generalization in vision: A survey. *arXiv preprint arXiv:2103.02503*, 2021. [6](#)
- [81] Kaiyang Zhou, Jingkang Yang, Chen Change Loy, and Ziwei Liu. Learning to prompt for vision-language models. *International Journal of Computer Vision*, 130(9):2337–2348, 2022. [7](#)
- [82] Zhilin Zhu, Xiaopeng Hong, Zhiheng Ma, Weijun Zhuang, Yaohui Ma, Yong Dai, and Yaowei Wang. Reshaping the online data buffering and organizing mechanism for continual test-time adaptation. In *Proc. European Conference on Computer Vision (ECCV)*, 2024. [1](#), [2](#), [8](#), [12](#), [14](#)